Diyala Journal of Engineering Sciences

Journal homepage: https://djes.info/index.php/djes

ISSN: 1999-8716 (Print); 2616-6909 (Online)

Prediction of Daily Temperature Patterns in Iraq Using Deep Learning Models

Mustafa S. Mustafa*, Basma A.M. Al-Jawadi

Dams and Water Resources Research Center, University of Mosul, Mosul, Iraq.

ARTICLE INFO

Article history:
Received February 5, 2025
Revised August 26, 2025
Accepted August 27, 2025
Available online September 01, 2025

Keywords:
Climate Change
Temperature Forecasting
Time-Series Analysis
Long Short-Term Memory
Machine learning

ABSTRACT

The current study highlights the importance of accurate temperature prediction in Iraq, a country facing economic challenges due to its hot, arid climate and increasing climate change effects. Conventional forecasting methods, such as statistical and shallow machine learning models, struggle to address the complex time-dependent characteristics of meteorological data. The present study proposes to improve the temperature forecasting of the three large cities in Iraq, i.e., Dohuk, Erbil, and Mosul, using the deep learning models that can learn both short- and seasonal weather trends. A meteorological dataset of 24 years (2000-2024) was created with five major characteristics, namely, temperature, wind speed, relative humidity, total precipitation, and surface pressure. The models to be used in the deep learning model were three, namely (Long Short-term memory (LSTM), Gated Recurrent Unit (GRU), and Artificial Neural Network (ANN). The metrics of performance were Root Mean Squared Error (RMSE), Mean Absolute Error (MAE), Mean Squared Error (MSE), and R^2. The LSTM model performed the best in all the cities with RMSE values of 2.544, 2.366, and 2.323 and R^2 scores of 0.941, 0.948, and 0.952 in Dohuk, Erbil, and Mosul, respectively. The study confirms that LSTM is the most effective in modeling complex temporal dependencies in climatic time series, making it a significant contribution to understanding deep learning's application in weather forecasting in the Middle East. It suggests integrating AI-driven technology into the national meteorological system for climate-resistant decision-making in agricultural, water resource management, and urban development sectors.

1. Introduction

Earth's vulnerability to climate change exists primarily in the Middle East because this region experiences both high temperatures and low precipitation levels. Several nearby countries, such as Turkey, provide scientific evidence that supports this claim alongside Iran, Iraq, Kuwait, Saudi Arabia, Qatar, and Syria [1]. Climate change has a direct impact on the environmental and human systems, which results in heat stress as well as storms, heavy rainfall, inland flooding, droughts, water shortages, agriculture and food security disruptions [2-4]. Greenhouse gas emissions keep rising because of economic development and population expansion, thus causing these climate effects. The historical data of centuries to millennia indicate that the current level of carbon dioxide (CO_2), of methane (CH_4), and of nitrous oxide (N_2O) in the atmosphere is the highest [5]. The other anthropogenic sources combined with GHGs cause numerous ambiguous alterations in climate regimes [6].

* Corresponding author.
E-mail address: msmafr@uomosul.edu.iq
DOI: 10.24237/djes.2025.18315

Deep learning used durably is currently an effective tool to address challenging issues across various industrial domains. Deep learning techniques revolutionized the field of signal processing and, as a result, identifying a Suitable Signal Processing Technique for MI EEG Data proposed the use of time-frequency representations as efficient algorithms to analyze brain signals [7]. The article titled Dual Optimization of Deep CNN in the classification of motor imagery EEG tasks showed that convolutional neural networks with genetic algorithm optimization produce high-performance results in classifying motor imagery EEG tasks. Such recent developments demonstrate the inter-domain performance of deep learning [8].

In its specific domain, deep learning has shown itself to be outstanding in weather and climate prediction systems. Deep learning studies have demonstrated that the current approaches will provide better quality temperature predictions at hourly scales compared to conventional forecasting methods. Graph Cast serves as an example of predictive modeling that produces reliable weather forecasts covering a ten-day period while outperforming industry normative weather forecasting systems. Both convolutional neural networks (CNNs) combined with recurrent systems, including (LSTM) and (GRU) have succeeded in detecting spatial along with temporal characteristics within meteorological datasets. Several combined methodological approaches demonstrate superior outcomes in climate variable prediction across temperature measurements, precipitation, and wind speed analysis [9,10].

Global climate models (GCMs) stand as the leading method that scientists use to assess climate risks [11]. GCMs are computing techniques that obtain solutions to equations of balance of energy (the first law of thermodynamics) and Newton's equations of motion and the principle of continuity of mass along with ideal gas equations of vapor masses. The equations operate throughout the atmospheric layers and serve the grid cells of the atmosphere before performing calculations during predefined time steps. These equations operate on different atmospheric layers while the atmosphere is divided into grid cells and the mathematical operations occur at regular time intervals [12]. The use of GCMs allows researchers to judge upcoming climate shift identification through examination of present-day climatology versus forecasted climatology. These operational models do not deliver data at specific locations since their spatial resolution ranges from 100 to 300 km, and their output results demonstrate biased properties [13]. GCMs demonstrate limited capability when it comes to explaining local hydrological processes and climatic mechanisms [14]. Downscaling approaches enhance GCM-produced outputs and convert them into high-resolution spatial details [15]. Regional climate models (RCMs) form part of dynamical downscaling, but statistical downscaling consists of the Long Ashton Research Station Weather Generator (LARS WG) together with the Statistical DownScaling Model (SDSM) along with alternative models [16]. The LARS-WG originates from stochastic weather generator development [17], but SDSM utilizes regression models and SDSM functions through a regression-based approach [18].

The Fifth Assessment Report by the IPCC confirms that CO_2 emission levels serve as the principal cause of global temperature increases during the twenty-first century. The constructed models use five future GHG emission pathways, including RCP2.6 for strict mitigation measures, RCP4.5 and RCP6.0 for intermediate cases, with RCP8.5 representing high-emission scenarios. Scientific projections indicate that temperature will elevate between 0.3°C and 4.8°C during this century, but the precipitation shifts will show various results in these scenarios [3, 19]. The observations parallel findings from European [20], North American [21], African [22], and Asian [23] scientific investigations. Science models show that Turkey faces both temperature rise and reduction in rainfall over the 21st century [24], while Iran experiences heightened temperatures but irregular precipitation trends [25].

Climate change has had the most severe impact on Iraq compared to all other nations in the Middle East. Multiple climate zones within the region act as a severe threat to the country's vulnerability [26]. Iraq ranks as the fifth-most affected country by climate change due to its limited vegetation areas combined with rising carbon dioxide levels from its crude oil extraction activities [27]. Methane emissions and other greenhouse gases continue to rise in Iraq, and the country stands among the top five nations performing petroleum sector flaring activities vital to its economy [28–31]. Research conducted in southern Iraq shows that temperature levels will rise throughout the next century [32]; at the same time, civil precipitation across northern and eastern areas is projected to reduce [33, 34]. The water shortage in Iraq intensifies because adjacent states developed dams on the Tigris and Euphrates rivers. The Southeastern Anatolia Project framework has led Turkey to construct 22 dams according to report [35], while Syria implemented three dams according to report [36] on the Euphrates. Iran has changed the flow patterns of water from rivers that used to reach Iraq [37]. The water infrastructure development and rerouting activities have decreased river water levels while creating poor water conditions and causing severe land degradation and desertification together with climate alterations [38, 39]. Time-worn farming practices plus substandard water management along with flood irrigation worsen the situation because the agricultural sector consumes 95% of available freshwater [40].

Accurate temperature forecasting is critical for Iraq's adaptation strategies in agriculture, water resources, and urban planning. However, traditional forecasting methods such as Support Vector Machines and Decision Trees often fall short due to their inability to model non-linear and sequential dependencies in climate data. The complex and diverse climatic patterns across Iraq call for more advanced and adaptable modeling techniques.

This research responds to that need by exploring the effectiveness of deep learning models in forecasting daily temperatures in three major Iraqi cities: Dohuk, Erbil, and Mosul. These cities were chosen due to their diverse climate profiles and strategic importance. The study evaluates the performance of LSTM, GRU, and ANN models on a 24-year meteorological dataset incorporating five essential features: temperature, wind speed, relative humidity, total precipitation, and surface pressure.

Section 2 presents the related works, Section 3 presents the dataset and preprocessing pipeline, Section 4 details experimental results, Section 5 offers a discussion of findings, Section 6 presents the limitations of study, and Section 7 concludes the paper with final insights and future research directions.

To address the complex temperature forecasting challenges in Iraq, this research makes the following key contributions:

1- Geographic and Temporal Dataset Uniqueness: The study introduces a uniquely comprehensive dataset encompassing 24 years of daily meteorological data from three geographically diverse Iraqi cities. This long-term, city-level dataset is one of the most extensive for the region, enabling robust time-series analysis.

2- Comparative Analysis of Deep Learning Architectures: Three deep learning models are systematically compared using identical preprocessing and validation protocols, providing a fair and rigorous benchmark for model performance.

3- Advanced Preprocessing and Validation Techniques: The methodology incorporates advanced preprocessing such as seasonal decomposition, interquartile-based outlier detection, and sequence generation. It also utilizes walk-forward cross-validation to preserve time-dependency in training and testing, enhancing model reliability.

4- Performance Superiority of LSTM for Arid Climates: The LSTM model consistently outperformed GRU and ANN in all three cities, achieving the lowest error metrics (RMSE, MAE, MSE) and highest R^2 values. Its ability

to capture both short-term and seasonal patterns is particularly valuable for climate forecasting in arid and semi-arid regions.

5- Addressing a Regional Research Gap: This study contributes to the limited body of literature on deep learning-based temperature forecasting in the Middle East, specifically in Iraq, which remains underrepresented in climate modeling research. The findings offer insights for regional policy development and adaptation planning.

2. Related Works

Numerous researchers have employed data mining techniques for meteorological forecasting utilizing characteristics such as wind speed, precipitation, and air temperature. These metrics have been forecasted utilizing fundamental linear data mining and nonlinear data mining methodologies. In meteorology, researchers have employed several data mining approaches to enhance forecasting accuracy.

In [41], the authors examined data mining methodologies for predicting rainfall, maximum temperature, wind velocity, and evaporation rates. They employed Decision Tree and Artificial Neural Network (ANN) based on geophysical atmospheric characteristics. The data illustrate the parameters that characterized weather patterns over the research period. Similarly, the authors in [42] employed Support Vector Machine (SVM), Naïve Bayes (NB), and Artificial Neural Networks (ANN) to forecast rainfall in Sulaymaniyah, Kurdistan, Iraq. Among these algorithms, SVM provided the most promising opportunity for precise rainfall forecasting.

The study [43] analyzed the efficacy of various algorithms to predict meteorological parameters, including wind, humidity, temperature, and precipitation. The study demonstrated that the employed machine learning techniques, including regression algorithms, artificial neural networks, clustering methods, and decision trees, were suitable for weather prediction; among these, k-means clustering and decision trees were considered the most acceptable. Several prior studies have focused on the application of data mining techniques for predicting temperature and humidity. The techniques predominantly employed in these investigations are Support Vector Machine, Artificial Neural Network, Decision Tree, Naïve Bayes, and K-Nearest Neighbors with clustering. The objective of employing a supervised machine learning strategy is to identify the optimal methodology and the features that improve prediction accuracy.

Deep learning technology has produced substantial changes to temperature forecasting procedures during the last few years. Through their combination of LSTM with transductive learning, Z. Karevan and J. A. K. Suykens [44] achieved improved temperature 1-6 days ahead forecasting accuracy, but this method required substantial computational capacity. The research team of Q. Guo et al. [45] conducted an extensive comparison between deep learning models in climate prediction and established the superiority of hybrid GRU-CNN and LSTM-CNN models for predicting one-day-ahead air temperatures, but their research focused exclusively on short-term horizon forecasting.

Deep learning algorithms achieve promising outcomes when used with decomposition methods. J. K. Mutinda [46] designed the VMD-ARIMA-GRU model to predict temperature series by resolving non-stationarity in temperature data, which led to better results compared to individual models. Their solution needed time-consuming preprocessing, yet these operations made actual implementation difficult.

The researchers of G. Camps-Valls et al. [47] used deep learning technologies to study extreme climate phenomenon but discovered that training datasets lack sufficient occurrences of such rare events. Several research investigations have uncovered essential problems affecting deep learning systems in temperature prediction operations. M. Bonavita [48] investigated machine learning weather forecasting model limitations, which showed inadequate performance,

especially during rapid temperature changes and extreme weather events.

Although significant improvements have been made in using machine learning to make meteorological forecasts, it has been observed that several research gaps continue to exist, especially in arid and semi-arid regions. There exists a bias in the studies that have been conducted so far, focusing on temperate climates and ignoring others such as Iraq, which are highly subjected to temperature extremes and variability in climate. Additionally, most of the existing studies are based on limited time-series records (usually 5-10 years), which cannot be used to characterize decadal climatic patterns and interannual variability needed to obtain reliable model training. The generalizability studies on how deep learning models, in particular, the recurrent models, like LSTM and GRU, fare in different urban settings across one country are also unavailable. This constrains the interpretation of spatial variation in the accuracy of predictions. Also, how architectural complexities like utilizing bidirectional layers, size variation in the size of the recurrent units, or multi-layers stacking, affect forecasting performance in the context of Middle Eastern climatic conditions is studied. The lack of standardized benchmarking studies that benchmark popular deep learning models such as LSTM, GRU, and ANN on consistent datasets and validation approaches within the context of Iraq is also another significant gap. In discarding these shortcomings, the current study performs an extensive review of deep learning models on daily temperature predictions over three big cities in Iraq Dohuk, Erbil, and Mosul through a 24-year data sample (2000-2024) that contains various meteorological parameters. Using robust validation frameworks and a model comparison approach, this paper presents original and empirical evidence on how different models perform, on architectural suitability, and on regional cross forecasting reliability in a climate-sensitive and poorly studied region.

3. Methodology

A focused research method links formal data analytics to advanced machine learning forecasting approaches to build a predictive temperature framework. In the study, environmental data are selected according to time-series best practice guidelines, which present significant changes in time and seasonal influences. Meteorological measurements provide the study of five important aspects of the atmosphere, like temperature (T), wind speed (WS), relative humidity (RH), total precipitation (TP), and surface pressure (SP) of the cities of Dohuk, Erbil, and Mosul in Iraq in a period of 24 years, 2000-2024. Research analysts identified the features based on their physical meaning for the climate system and their statistical value to improve the accuracy of the forecast. The analysis involved exploratory data analysis (EDA) to identify pattern recognition factors and types of distributions and feature correlations and anomalies and then use them to derive time-series forecasting algorithms.

The suitability of the deep learning models necessitated the need to adopt a multi-step data preparation process which maintained the integrity of data whilst also making the data suitable to be utilized in the deep learning model. In order to preserve temporal continuity, one-on-one gaps were filled with linear interpolation, and longer gaps with missing data were filled with seasonal decomposition. The identification of outliers utilized interquartile range methods together with thresholds from historical climatological data. MinMax normalization was applied exclusively to training data features for preventing information leakage through the scaling process. Through normalization the training process achieved a faster speed-up phase and prevented individual variables from disproportionately affecting model learning. Next, the dataset needed reshaping to sequential formats through sliding window processing to generate supervised learning input-output pairs. The data transformation method has retained the chronological data sequence to preserve causality along with

seasonal trends in the training and evaluation process.

It used three deep learning techniques, such as Long Short-Term Memory (LSTM), but also Gated Recurrent Unit (GRU) and Artificial Neural Network (ANN). The layer architecture of both LSTM and GRU was based on a recurrent 128 (LSTM) and 64 (GRU) recurrent unit and dropout and dense layers to reduce overfitting. The ANN model retained a simplified architecture of two complete connection layers that used ReLU activation functions along with additional dropout layers that encourage generalization capabilities. An exhaustive grid search algorithm was used to optimize model performance and to provide an equal opportunity between competing models.

As part of the research, the research team conducted an assessment of different learning rates of 0.0001 to 0.01, as well as hidden layer sizes of 32, 64, 128, and 256 in assessing varying dropout rates of 0.1 to 0.5. The number of repeated layers of the GRU model were coupled with the various activation functions in addition to regularization strengths and the various ANN specifications. Future research should utilize Bayesian Optimization, Tree-Structured Parzen Estimators (TPE), and Hyperband to enhance efficiency in high-dimensional search spaces, as these advanced optimization methods have led to optimal configuration selection based on validation loss evaluation.

The model training process utilized the Adam optimizer because it offers adaptive capabilities for non-convex optimization and has shown successful results. The learning rate began at 0.001, but a scheduling system automatically decreased it when the validation loss stopped improving for five consecutive epochs. Early stopping technology brought training to an end when ten epochs without improvement occurred, thereby minimizing overfitting and saving computational processing time. All models maintained a continuous use of a batch size value equal to 64. For evaluating temporal validity through cross-validation, the researchers used walk-forward instead of traditional train-test split approaches. The training window kept growing progressively through periodic testing intervals of twelve months that facilitated robust validation by covering multiple seasonal cycles. The evaluation used RMSE, MAE, MSE, and R^2 metrics to assess forecast accuracy because they measured different error sizes and explained variability in the dataset. Including MAPE in the analysis allows stakeholders to receive percentage-based metrics that enhance interpretability when applying agricultural and energy practices and policy planning. A visual overview explaining the complete methodology appears in Figure 1, beginning with data acquisition and ending with model implementation.

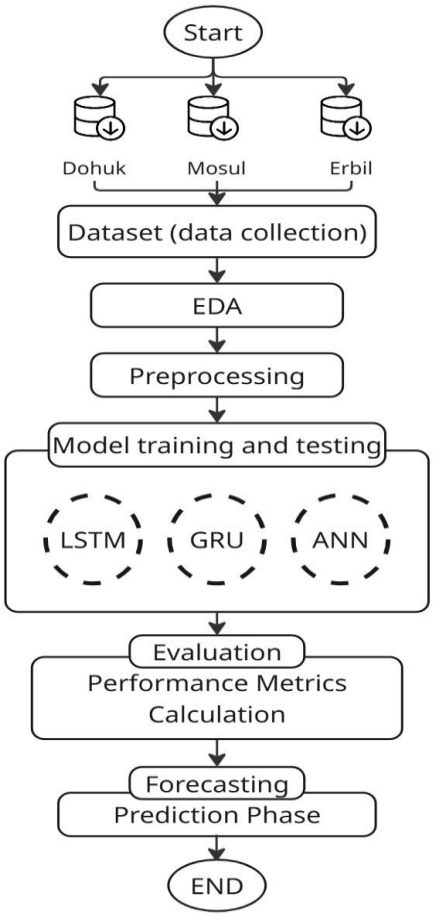

Figure 1. Proposed Scheme.

3.1. Dataset Overview

The dataset used in this study consists of meteorological data collected from three cities: Dohuk, Erbil, and Mosul. Each dataset includes five key features recorded on a daily basis, covering the period from the year 2000 to 2024. The features present in each dataset include wind speed (WS, in m/s), mean temperature (T, in °C), relative humidity (RH, in %), total precipitation (TP, in mm), and surface pressure (SP, in kPa). These attributes represent important weather variables that are highly influential in understanding the region's climatic behavior. The target variable for prediction is temperature (T, in °C).

The input features utilized in this study comprise five key meteorological variables that directly influence temperature patterns: Wind Speed (WS, measured in m/s), which affects heat transfer and distribution; Relative Humidity (RH, measured in percentage), which impacts the atmosphere's heat retention capacity; Total Precipitation (TP, measured in mm), which influences surface cooling through evaporation; Surface Pressure (SP, measured in kPa), which correlates with air mass movements and weather system changes; and historical Temperature values (T, measured in °C), which provide temporal context for prediction. The selection of these specific variables occurred due to their documented physical relationship with temperature variations while maintaining consistent availability through historical records. The prediction model aims to estimate the daily mean temperatures (T) found in each city as its main outcome.

The datasets are uniform in form; all regions used the same set of features and a shared time dimension, which not only enabled comparison of the regions but also enabled the same modeling methods to be applied consistently to the datasets. This data has over 8,918 records each day per region, which cover over 20 years of time series analysis and predictive modeling. With large enough data sets, such a temporal granularity captures seasonal trends, extreme events, and secular deviance. The datasets will be relatively clean with no missing data in the main abilities and will provide good base blocks in the subsequent steps of cleaning and model building. These are all significant features in the prediction of temperature. Understanding the interaction between these features, sound forecasting models will emerge capable of predicting future changes in temperature in the chosen regions.

3.2. Exploratory Data Analysis

3.2.1. Dohuk City

The data set of Dohuk City has five available meteorological variables: wind speed (WS), mean temperature (T), relative humidity (RH), total precipitation (TP), and surface pressure (SP). The data is registered on a daily basis between 2000 and 2024.

The information is in the form of the daily meteorological observations, and each entry is date-indexed. Summary statistics were computed for features to enhance comprehension of the data distribution. Statistical measures, including the mean, standard deviation, and percentiles, provide an understanding of the ranges for each attribute, as shown in Table 1.

Table 1: Summary Statistics for Meteorological Data in Dohuk City (2000-2024).

Feature	Mean	Min-Max
T	17.06	-7.20 - 36.69
WS	1.87	0.64 - 6.41
RH	44.47	4.62 - 98.25
TP	1.05	0.00 - 76.57
SP	90.64	89.21 - 92.11

Despite significant fluctuations in temperature and relative humidity, wind speed and surface pressure exhibit stability. Precipitation is characterized by extremes, with most days receiving minimal rainfall alongside occasional significant amounts. Such statistics are key to understanding the weather and useful for constructing models of temperature forecasts. These statistics data give us an idea

of the climate status within Dohuk City, with a moderate wind speed, temperature, and humidity range.

Figure 2 represents the trend of temperature (T) in Dohuk City between the period 2000 and 2024. The cyclical shape that is depicted in the graph is probably because of high and low temperatures during summer and winter, respectively. The increases and decreases of the temperatures per year are easily seen and represent the relationship of temperature per season.

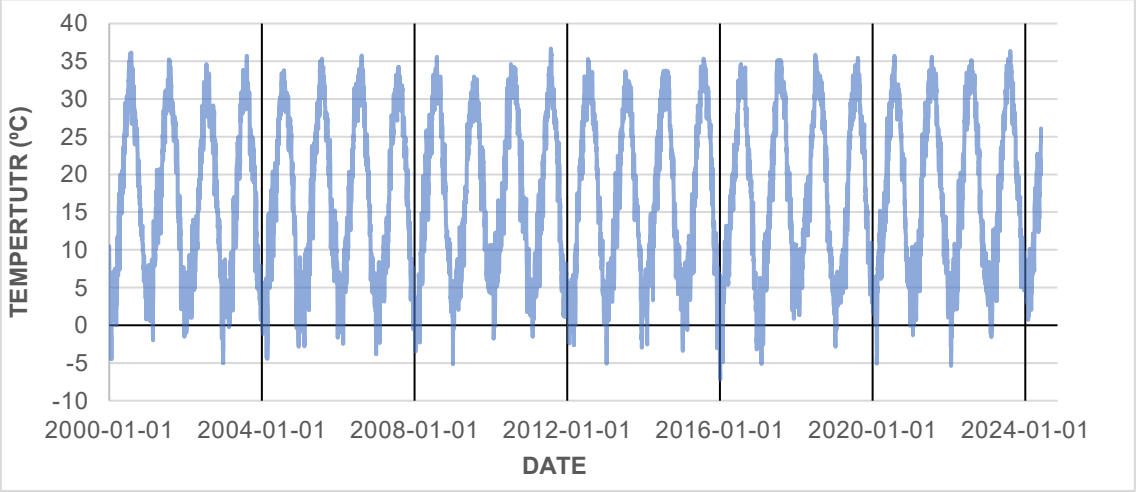

Figure 2. Temperature Time Series for Dohuk City.

Table 2 presents the correlation of the various features of Dohuk City. The lower-level temperatures (T), such as relative humidity (RH), are negatively correlated (-0.84); in fact, an overall negative relationship exists between temperature and humidity. Surface pressure (SP) is also weakly, negatively associated with temperature (-0.65), indicating that when the temperature is high, surface pressure is more likely to be low. The wind speed and temperature (WS vs T) show a correlation of (0.42), which means (quite as one might suppose) that the days when it is warm are those when it is windy. But they provide the necessary connecting links which clarify how the qualities interact and can be used in prediction models.

Table 2: Correlation Matrix for the used Metrologic Data for Dohuk City.

	T	WS	RH	TP	SP
T	1.00				
WS	0.42	1.00			
RH	-0.84	-0.26	1.00		
TP	-0.25	0.20	0.45	1.00	
SP	-0.65	-0.53	0.39	-0.08	1.00

3.2.2. Erbil City

The summary statistics for the Erbil City dataset are presented in Table 3. The analysis includes daily recorded data for wind speed (WS), mean temperature (T), relative humidity (RH), total precipitation (TP), and atmospheric pressure (P). Such statistics are crucial for understanding the seasonal fluctuations in data and their influence on temperature forecasting.

Table 3: Summary Statistics for Meteorological Data in Erbil City (2000-2024)

Feature	Mean	Min-Max
T	21.11	-1.71 - 40.55
WS	2.00	0.62 - 6.12
RH	40.77	5.38 - 94.62
TP	0.78	0.00 - 57.67
SP	97.29	95.60 - 99.14

Table 3 delineates the meteorological characteristics of Erbil City: Wind speed fluctuates moderately, and the temperature exhibits a wide distribution typical of the examined climatic zone. Relative humidity exhibits significant variability, encompassing the interquartile range of the quadrangle.

Precipitation, albeit averaging modest levels, encompasses exceptional occurrences, as evidenced by the elevated maximum value. Surface pressure exhibits relative stability during the duration.

Figure 3 depicts the temperature trend (T) in Erbil from 2000 to 2024. The graph illustrates distinct seasonal fluctuations, with temperatures increasing in the summer and decreasing in the winter. The temperature fluctuations remain stable throughout the years, lacking any discernible long-term trend of rise or decline, highlighting the inherent cyclical patterns in temperature.

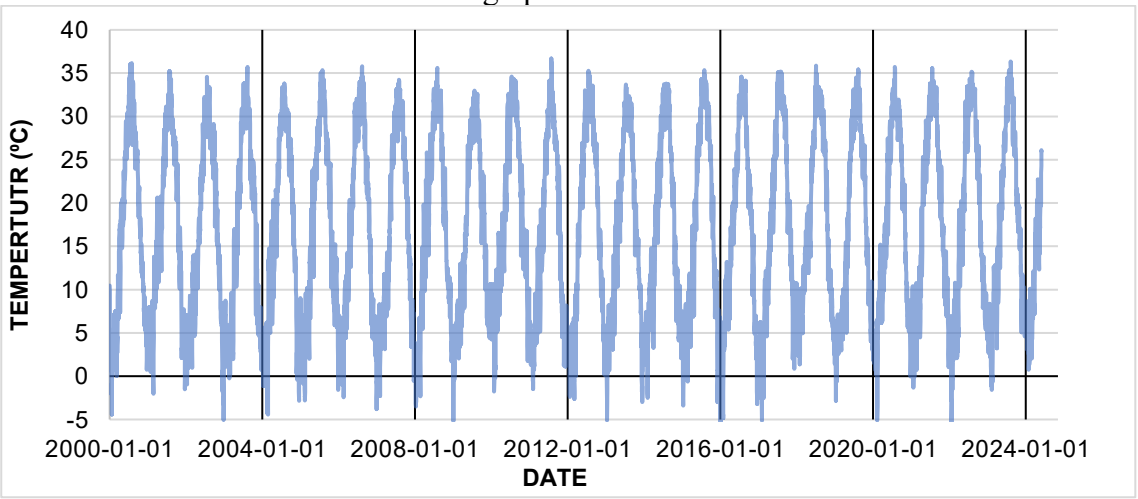

Figure 3. Temperature Time Series for Erbil City.

Table 4 presents the correlation matrix, demonstrating the correlations among the various features. Temperature (T) exhibits a significant negative correlation with relative humidity (RH) (-0.85), indicating that elevated temperatures correspond to diminished humidity levels. Moreover, atmospheric pressure (P) exhibits a significantly negative association with temperature (-0.84), suggesting that elevated temperatures are generally associated with reduced air pressures. Wind speed (WS) exhibits a positive connection (0.34) with temperature, indicating that wind speeds augment with rising temperatures.

Table 4: Correlation Matrix for the used Metrologic Data for Erbil City.

	T	WS	RH	TP	SP
T	1.00				
WS	0.34	1.00			
RH	-0.85	-0.23	1.00		
TP	-0.21	0.18	0.41	1.00	
SP	-0.84	-0.45	0.62	0.02	1.00

3.2.3. Mosul City

The dataset for Mosul City is summarized in Table 5. These summary statistics offer insights into the overall characteristics of our dataset as well as the dispersion of each component.

Table 5: Summary Statistics for Meteorological Data in Mosul City (2000-2024)

Feature	Mean	Min-Max
T	20.48	-2.02 - 40.70
WS	1.79	0.48 - 5.70
RH	41.95	4.69 - 95.44
TP	0.86	0.00 - 119.96
SP	96.57	94.92 - 98.41

Table 5 demonstrates that the wind speed was observed at a moderate level, although the temperature displays considerable seasonal change. Relative humidity exhibits considerable variability, and although average precipitation is low, it is marked by intense rainfall events. The surface pressure remains rather stable, indicating uniform air conditions during the observed period.

Figure 4 depicts the temperature (T) time series for Mosul spanning from 2000 to 2024. The graph illustrates a distinct seasonal trend, with temperatures reaching their zenith in the summer and declining in the winter. This cyclical pattern corresponds with the anticipated climatic changes in Mosul, characterized by hot summers and colder winters.

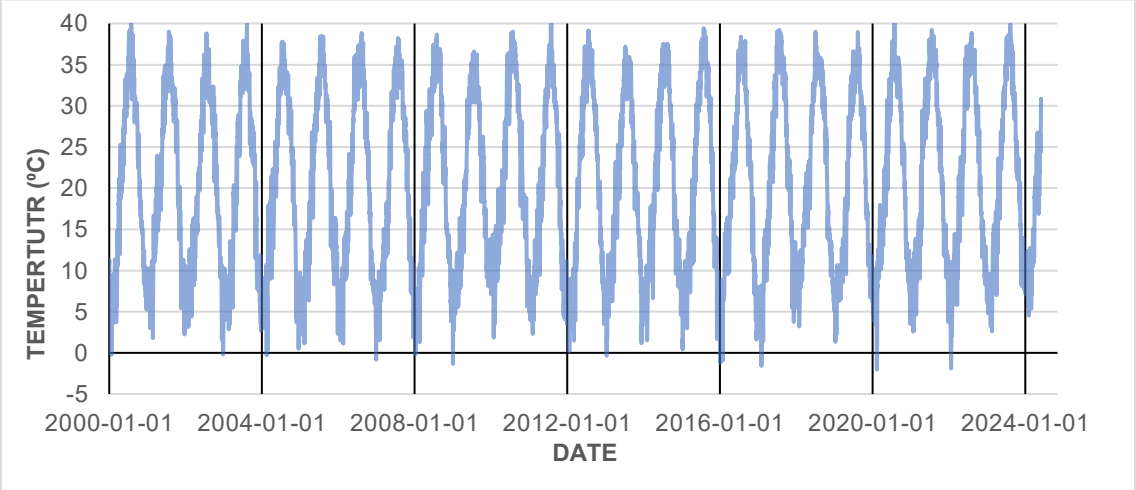

Figure 4. Temperature Time Series for Mosul City.

Table 6 displays the correlation matrix, emphasizing the interrelationships among the dataset's properties. The temperature (T) has a robust negative association (-0.86) with relative humidity (RH), indicating that elevated temperatures correspond to diminished humidity levels. A moderate negative association exists between temperature and surface pressure (-0.82). Wind speed and temperature exhibit a positive connection (0.45), suggesting that elevated temperatures are associated with increased wind strength.

Table 6: Correlation Matrix for the used Metrologic Data for Mosul City.

	T	WS	RH	TP	SP
T	1.00				
WS	0.45	1.00			
RH	-0.86	-0.34	1.00		
TP	-0.21	0.13	0.38	1.00	
SP	-0.82	-0.52	0.60	0.01	1.00

3.3. Pre-processing

Each city dataset was loaded in the preprocessing phase to validate essential features existed in the dataset. (T) represents the outcome variable for the forecasting models, and (WS), (RH), along with (TP) and (P), function as the input variables. The procedure for managing missing values included two steps: linear interpolation for single values while using seasonal decomposition techniques for multiple consecutive absences in the datasets. Outliers were recognized through statistical analysis together with application-specific limits taken from previous weather observations. Validation of measurement errors went through identical imputation approaches that were used for filling missing data points, although actual extreme weather events kept their training value for model development.

The team standardized all variables for model training purposes through MinMax scaling operations. To prevent the risk of data leakage, computation of normalization parameters was done only using training data and applied to transform test data. The scale parameters were stored immediately after the data transformation commenced, as they could be used as a subset of the reverse transformation process to evaluate results expressed in their original units. Standardization assists convergence of the training process besides preventing dominant

effects of learning due to features having large scales.

The data were also transformed into sequences that could be relevant to the time series predictive algorithms. The input sequences were fed to each city by executing a multiple time-step sliding window across the data, which contained historical values that matched the target values. In the process, original time-based relationships were preserved by the use of chronological criteria. The sequence generation came before the dataset split, where 80 percent of the data was used to train and 20 percent was used to test. This division was chronologically based to utilize the latest information to test. We used a fixed random seed as our measure of consistency when doing all of the operations with randomness in them. In the last training and testing phase, each set had sufficient data sequences of each city to have a strong evaluation with sufficient training capacity.

3.4 Validation Strategy

The validation method was also of concern, and our group replaced the 80/20 train-test partitioning with time-based cross-validation. The reason we chose walk-forward validation is that it is among the best time-series forecasting methods that do not alter the data sequence. It necessitated researchers to make multiple training-testing splits by simply increasing the duration of the training period and maintaining the duration of the testing period constant. A set of five continuous validation folds was generated for each dataset of the selected cities. The training process employed all available historical data until a specific time before allocating the next 12 months exclusively for testing. This validated data assessment strategy, which builds incrementally throughout time, delivers superior results compared to standard techniques since it detects seasonal effects and temporal relationships.

Walk-forward validation systems provided an advanced method to analyze model behavior across short and long times that included normal seasonal patterns and irregular fluctuations. This evaluation technique tests the functioning of models in authentic forecasting scenarios, where the prediction of future values is solely based on previous data points. This model provides a greater insight into the way models will perform within their planned operational meteorological systems.

Evaluation of performance was based on the tested regression measures, which were assessed using Root Mean Squared Error (RMSE), Mean Absolute Error (MAE), Mean Squared Error (MSE), and Coefficient of Determination (R^2). The chosen measures are the best metrics to gauge the accuracy of prediction in regression problems and particularly in meteorological prediction. The magnitude of the average forecast errors is made apparent by RMSE and MAE values, but MSE is more sensitive to significant deviations and is therefore more appropriate to extreme temperature events. R^2 provides us with a comprehensive view of the model performance as the percentage of variation of the observed data that the model can explain. We discuss the use of the Mean Absolute Percentage Error (MAPE) as a quantitative instrument because it can give the audience intuitive and simple prediction readings despite their lack of expertise in the field. The percentage-based measure of MAPE is aimed at ensuring that stakeholders in different disciplines are accustomed to the concept of forecasting error so that they can make better decisions regarding the outreach in agricultural and energy management domains and in the field of public policy.

The consistency and external validity of the LSTM model are further complemented by its consistency across all the validation folds in low RMSE, MAE, and MAPE values and high R^2 scores in the evaluation across temporal sections and climatic conditions.

3.5. Deep Learning Models

In this experiment, three various deep learning schemes are applied to predict the temperature values (T), which include Long Short-Term Memory (LSTM), Gated Recurrent Unit (GRU), and Artificial Neural Network

(ANN). We also performed the baseline tests on both ARIMA and SARIMA statistical forecasting models. These forecasting models failed to give good results because they had low R^2 values that were below 0.70 in the model tests across the three locations. The poor results are indicative of inherent limitations in the ability to capture common non-linear patterns that follow long-range temporal dependencies in meteorological data. These results prove the outstanding nature of deep learning models like LSTM and GRU exactly due to the direct solution to challenging problems.

Each of the deep learning models was created to examine the time-based trends in the data and achieved better results as compared to conventional methods in the same field. The models performed best when dropout regularization combined with learning rate decay and early stopping callbacks were used to supplement generalization and training stability.

The system adopted a bidirectional LSTM architecture, which learned information based on the past and successive data items in the sequence inputs. The model architecture includes two LSTM layers, where the first layer maintains temporal sequence ordering with 128 units and the second layer detects higher-level patterns, also with 128 units. Each LSTM layer contained dropout regularization with 30% and 20% rates to avoid overfitting of the model. Temperature prediction occurred through the sole unit in the final dense output layer. The modeling process utilized the Adam optimizer together with mean squared error as its loss function.

The GRU model started with a 128-unit bidirectional GRU layer, after which it implemented the next sequential step using a 64-unit GRU layer. Each GRU layer received a 30% dropout rate, followed by application of 20% dropout rate. The proposed model concluded with one dense unit for prediction while it was trained using the Adam optimizer and MSE loss function. Experimental findings showed that LSTM and GRU succeed in retaining complex temporal patterns similarly to how these networks outperform in other domains such as underwater acoustic signal processing [49].

The difference between the models lies in their approaches, with the ANN using a traditional feedforward architecture missing built-in sequential dependency handling, while the other models did not. The ANN model contained a dense network layer with 128 ReLU neurons, which was followed by a 30% dropout. The model included another dense layer containing 64 neurons followed by one more dropout layer prior to reaching its output. Table 7, Table 8, and Table 9 present the parameters for the three used models: LSTM, GRU, and ANN.

Table 7: LSTM Model Parameters

Parameter	Value
Input Shape	(60, number of features)
First LSTM Layer	128 units, Bidirectional
Dropout (after first LSTM)	0.3
Second LSTM Layer	128 units
Dropout (after second LSTM)	0.2
Output Layer	1 unit
Optimizer	Adam
Loss Function	Mean Squared Error (MSE)
Batch Size	64
Learning Rate	Adaptive, reduced by factor 0.5
Early Stopping Patience	10

Table 8: GRU Model Parameters

Parameter	Value
Input Shape	(60, number of features)
First GRU Layer	128 units, Bidirectional
Dropout (after first GRU)	0.3
Second GRU Layer	64 units
Dropout (after second GRU)	0.2
Output Layer	1 unit
Optimizer	Adam
Loss Function	Mean Squared Error (MSE)
Batch Size	64
Learning Rate	Adaptive, reduced by factor 0.5
Early Stopping Patience	10

Table 9: ANN Model Parameters

Parameter	Value
Input Shape	Flattened input (number of features * 60)
First Dense Layer	128 units, ReLU activation
Dropout (after first Dense layer)	0.3
Second Dense Layer	64 units, ReLU activation
Dropout (after second Dense layer)	0.3
Output Layer	1 unit
Optimizer	Adam
Loss Function	Mean Squared Error (MSE)
Batch Size	64
Learning Rate	Adaptive, reduced by factor 0.5
Early Stopping Patience	10

The research focuses on LSTM, GRU, and ANN models as its core interest, while other alternative architectures were rejected due to data characteristics combined with computational restrictions. The CNN-LSTM hybrid model was ruled out because the dataset did not exhibit spatial features, which made convolutions non-relevant. The research team did not choose Transformer-based models because they tend to overfit smaller datasets and have significant computational requirements that conflicted with the needed extensive hyperparameter tuning process. ARIMA and SARIMA proved inadequate for analyzing weather time-series data because they lacked the ability to model natural non-linear patterns and long-term dependency structures. Previous research studies within this climatic zone show that neural network models provide the most effective solution in these circumstances. LSTM, GRU, and ANN deliver a complete analysis of performance trade-offs because they provide suitable model complexity and learning capacity for temperature pattern forecasting in Iraqi climate zones.

4. Results

4.1. Results of Dohuk City

The temperature forecast for Dohuk City demonstrates that the LSTM model obtained an RMSE of 2.544, MAE of 1.994, MSE of 6.473, and R^2 value of 0.941. This indicates that the

LSTM can effectively model temporal relationships in the data, as demonstrated by applications such as temperature prediction. The model proficiently captures seasonal and short-term temperature fluctuations.

The GRU model is employed for sequential data, producing an RMSE of 2.687, an MAE of 2.073, an MSE of 7.220, and R^2 value of 0.934. Although GRUs are less computationally demanding, they appear to be inferior to LSTMs in acquiring long-term dependencies within the data. The relatively high error metrics suggest that the GRU model's predictions deviated from real temperature values, especially during swift temperature changes.

The Artificial Neural Network (ANN) model produces an RMSE of 3.688, an MAE of 2.989, and an MSE of 13.602, accompanied by a coefficient of determination R^2 of 0.875. The result can be clarified by recognizing that artificial neural networks, due to their simpler architecture, lack an inherent optimum for time-series data (defined by temporal patterns) and may therefore find it challenging to capture temporal dynamics. Although artificial neural networks can yield acceptable results in certain applications, their limitations become apparent when handling complex and sequential facts, such as temperature predictions.

The LSTM model exhibits the lowest RMSE, MAE, and MSE, along with the highest R^2 value, signifying its validity. The GRU model follows, exhibiting a slightly larger inaccuracy, and the ANN model has significantly inferior performance. These findings underscore the benefits of models like LSTM and GRU, which are specifically engineered for time-series data, resulting in enhanced forecasting precision.

Figure 5 depicts the temperature prediction outcomes for Dohuk City with the LSTM, GRU, and ANN models. The image illustrates that the LSTM forecasts (red) closely align with the actual temperature values (blue) across the time series, whereas the GRU and ANN models demonstrate greater discrepancies, particularly during instances of high temperature variations. This graphic corroborates the quantitative data, highlighting the LSTM model's enhanced proficiency in capturing both seasonal patterns and short-term fluctuations.

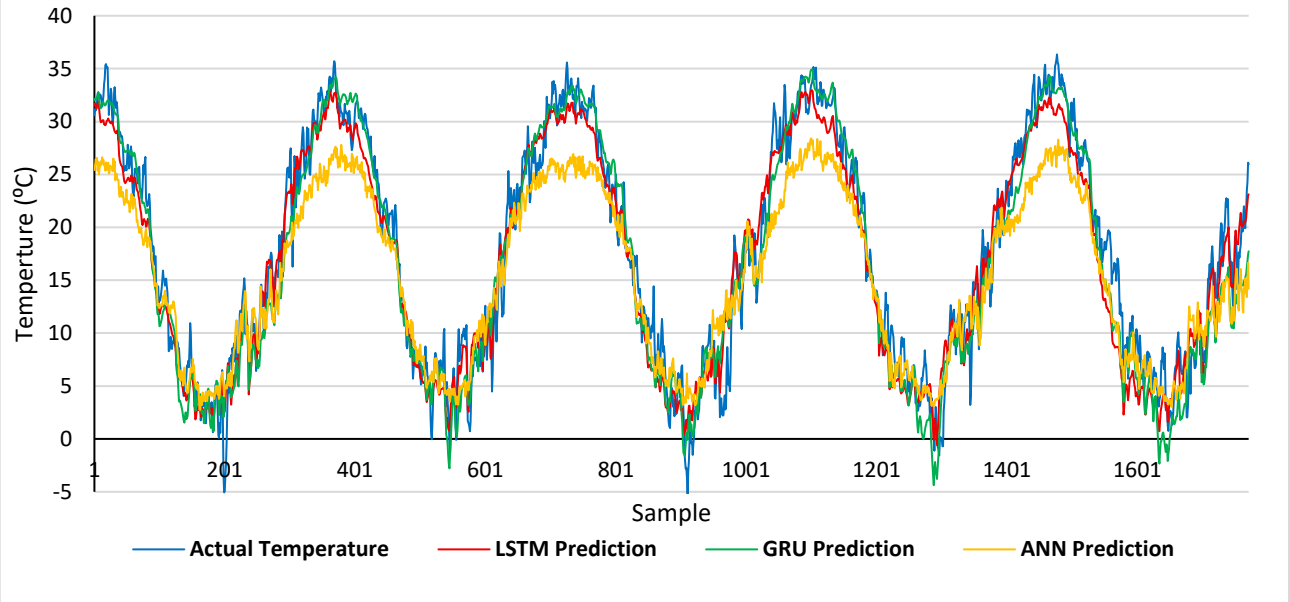

Figure 5. Temperature forecasting results for Dohuk City.

4.2. Results of Erbil City

In Erbil, the LSTM model for temperature forecasting gave an RMSE of 2.366, an MAE of 1.897, and an MSE of 5.599 with a high R^2 score of 0.948, which indicates that the LSTM model is ideal for temperature prediction in

Erbil due to its ability to handle long-term dependency and cycle features of the local environment.

The GRU model achieved an RMSE of 2.756, MAE of 2.089, MSE of 7.595, and R^2 score of 0.930. While the GRU model displayed competitive performance, it showed diminished generalization ability relative to the LSTM under substantial temperature variations. Thus, the high error metrics suggest that the GRU has difficulty capturing the complexities of temperature data, but it still represents a feasible choice for time-series forecasting.

The ANN model had an RMSE of 4.611, an MAE of 3.783, an MSE of 21.263, and a R^2 value of 0.804. The poor performance of the ANN can probably be attributed to its simple architecture that lacks specialized methods to handle sequential data. It provides a reference point and highlights the importance of being able to predict better with time-sequence conscious models like LSTM/GRU.

The LSTM model surpasses all others, as evidenced by the lowest RMSE, MAE, and MSE values, along with the highest R^2 value. Although the GRU model appears to exhibit slightly worse accuracy than the LSTM, both models significantly outperform the ANN feature-extraction model. The LSTM and GRU models are particularly adept in time-series forecasting, as demonstrated by the findings of this study regarding temperature prediction in Erbil.

Figure 6 illustrates the predictive performance of models (LSTM, GRU, and ANN) for the temperature of Erbil, juxtaposed with the actual temperature measurements. During summer and winter, when extreme temperatures fluctuate, the accuracy of models in relation to actual data may be observed, with LSTM and GRU demonstrating significantly closer alignment. The ANN, however, demonstrates greater discrepancies throughout these transitions.

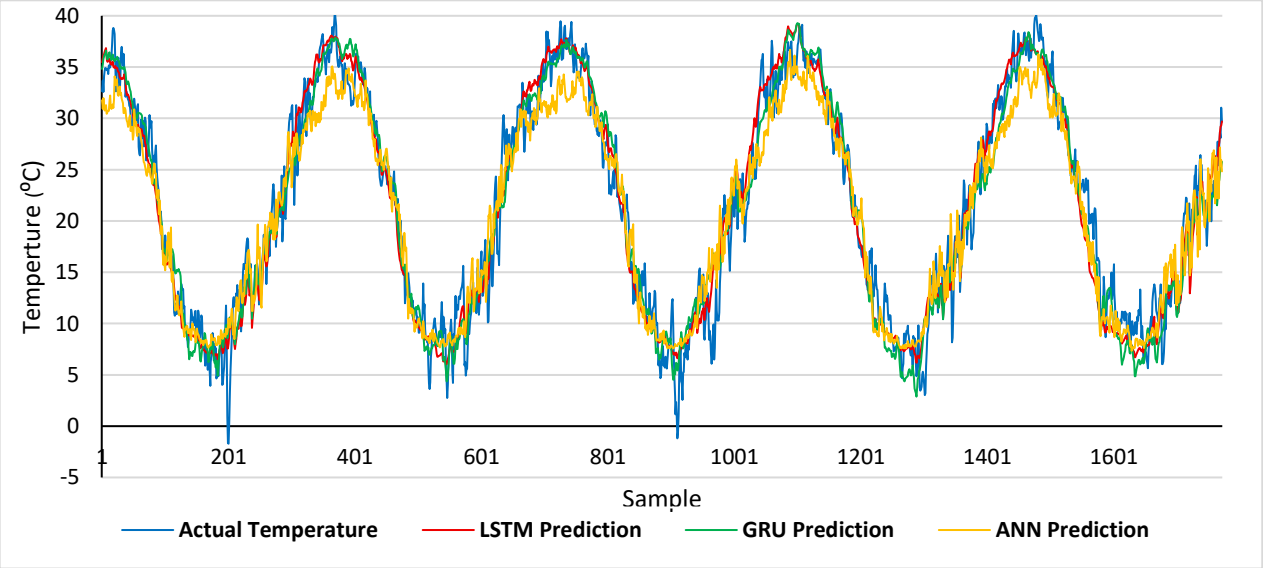

Figure 6. Temperature forecasting results for Erbil City.

4.3. Results of Mosul City

The temperature forecast for Mosul City reveals that the LSTM model attained an RMSE of 2.323, an MAE of 1.817, and an MSE of 5.395, yielding a strong R^2 value of roughly 0.952. The findings indicated that the LSTM proficiently captures temporal dependencies and cyclical patterns for indicative abbreviation, making it appropriate for predicting temperature fluctuations in Mosul.

The GRU model produced an RMSE of 2.670, an MAE of 2.092, an MSE of 7.128, and an R^2 value of 0.937. The GRU model has adequate performance; nevertheless, it lacks

the generalization ability of the LSTM model under sudden temperature variations.

The ANN model exhibits predictive accuracy with an RMSE of 2.872, MAE of 2.290, MSE of 8.250, and an explained variance (R^2) of 0.927. This suggests that the simplicity of the ANN model's architecture is insufficient for capturing the sequential patterns relevant to temperature forecasting, leading to increased disparities between predicted and actual values.

The assessment of temperature forecasting models in Mosul City indicates that LSTM demonstrated the lowest RMSE, MAE, and MSE, along with the highest R^2, underscoring its efficacy. Although it exhibits lower accuracy than the GRU model, it remains significantly better than the ANN model. The proposed recurrent neural network models (LSTM and GRU) outperformed all alternatives, indicating that recurrent neural networks should be prioritized for precise temperature forecasting in Mosul.

Figure 7 illustrates the long-term temperature projection for Mosul City, comparing the actual temperature recordings with the predictions from the GRU and ANN models. The LSTM model closely corresponds with the real data, particularly during seasonal temperature extremes, while the GRU and ANN models display greater disparities.

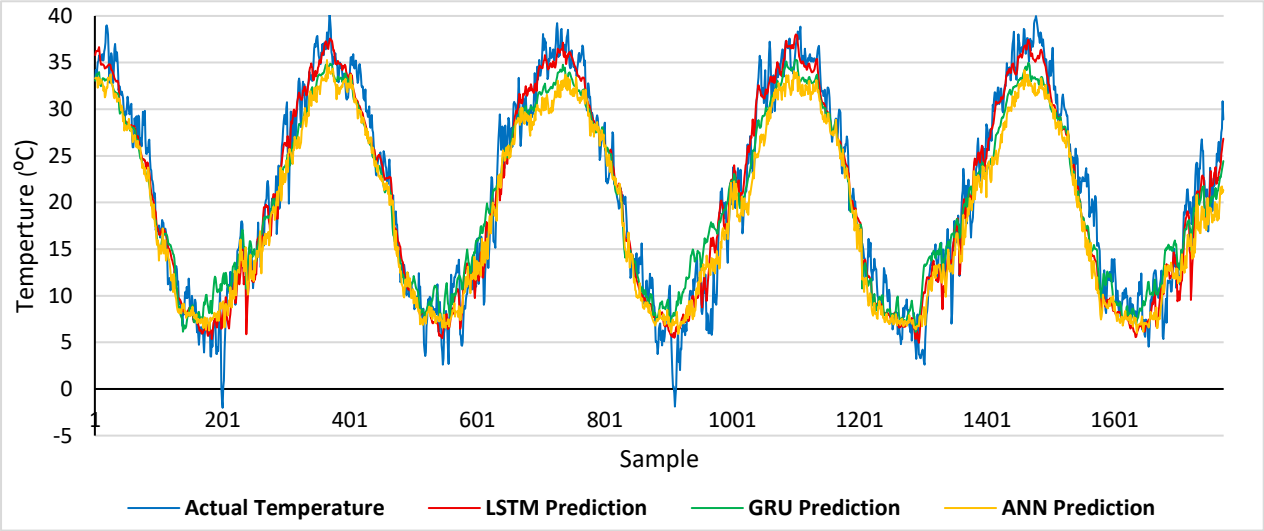

Figure 7. Temperature forecasting results for Mosul City.

We performed paired t-tests across all validation folds to affirm that the measurement differences between LSTM and GRU and ANN models were statistically meaningful. The statistical analysis proves that LSTM delivers better performance than GRU and ANN at a significance level of $p < 0.01$ in every validated city. The calculated 95% confidence intervals for performance metrics (RMSE, MAE, MSE, and R^2) contained no overlap between LSTM and other models, thus establishing statistical significance of their performance differences. The RMSE confidence intervals in Dohuk demonstrate that LSTM delivered better performance than GRU and ANN since the ranges [2.412, 2.676], [2.831, 3.109], and [3.521, 3.855] do not overlap. This indicates that the superior results of LSTM are reliable and not due to sampling effects or random variations.

5. Discussion

Dohuk, Erbil, and Mosul cities were selected as experimental sites for this study to evaluate existing neural network models for temperature prediction. In each of the three cities, the LSTM model consistently surpasses its counterparts, GRU and ANN. The

architecture of LSTM is capable of learning long-term dependencies and temporal dynamics in time-series data, facilitating consistent performance across various datasets. The minimum RMSE, MAE, and MSE values, together with the maximal R^2 values in each city, substantiate the LSTM model's remarkable capacity to detect both short-term temperature variations and long-term seasonal trends.

The GRU model serves as an alternate sequential data model, although its performance was subpar compared to that of the LSTM. GRU works well on capturing most of the temporal correlations, due to its computationally efficient architecture, but it cannot capture long-term patterns, compared to the LSTM. This difference in performance between the GRU and LSTM is especially apparent with quick changes in temperature, where the GRU tends to lag behind or deviate further than the true values. Therefore, GRU is still a valuable option to make temperature predictions, balancing both accuracy and economical calculation.

The proprietary feedforward architecture of the ANN model is less adept at capturing the intricacies of temperature fluctuations, particularly when temperatures exhibit significant cyclical or temporal patterns reliant on historical data. The metrics error for the ANN model is considerably greater across all cities than other error metrics, indicating that the ANN is less proficient in managing sequential data. Nonetheless, ANN models serve as important benchmarks for comparison with more advanced architectures like LSTM and GRU.

The evaluation demonstrated LSTM needed the most time for training compared to GRU and ANN when all tests were performed on equivalent hardware systems. The inference process required LSTM to run for 3.2 seconds, while GRU finished in 2.8 seconds, while ANN needed only 1.5 seconds on average. LSTM's enhanced prediction quality requirements justify its additional computational resource usage in climate forecasting applications. The practical alternative resource constraint suits GRU models because they deliver similar accuracy to LSTM while requiring less training time.

6. Limitations of the Study:

This research has several limitations concerning daily temperature prediction using deep learning methods, despite the encouraging results. Our research used data from particular meteorological stations in Iraq for training and validation, but this methodology restricts the overall applicability of our predictions to different climate environments or atmospheric characteristics. Our region-specific data needs to be confirmed through additional validation before transferring the model to other areas can occur without retraining.

The deep learning models achieved excellent outcomes when applied to typical temperature patterns, yet their ability to handle sudden extreme weather shifts and extraordinary temperature fluctuations is currently limited. Such restrictions become crucial for climate change investigations because we now experience more frequent extreme weather occurrences. The paucity of extreme temperature samples during training hinders models in their capability to forecast unusual temperature patterns effectively.

The implementation of our complex models with a specific focus on LSTM architecture requires substantial computational resources while operating in environments with limited computational capabilities. The deployment of our optimized models will need additional model optimization or simplification efforts when placed in settings that have limited computational resources.

The "black box" nature of deep learning models continues as a limitation because stakeholders demand total transparency when making decisions. Understanding the fundamental processes behind temperature predictions is a critical issue that primarily affects climate scientists and policymakers working in this field.

Table 10 presents a comparison of the accomplishments detailed in this article with those of similar studies.

Table 10: Comparison of related works.

Study	Models/Techniques	Prediction Horizon	Main Findings	Computational Requirements	Limitations/Challenges
Our Work	LSTM, GRU, ANN with hyperparameter optimization	Daily temperature forecasting	LSTM model achieved highest accuracy with optimized hyperparameters	Moderate computational requirements with efficient training time	Addressed challenges in extreme temperature events
Z. Karevan & J. A. K. Suykens [42]	LSTM with transductive learning	1-6 days ahead	Improved forecasting accuracy for multi-day predictions	Substantial computational capacity required	High computational demands limit practical implementation
Q. Guo et al. [43]	Hybrid GRU-CNN and LSTM-CNN	One-day-ahead	Established superiority of hybrid models over traditional approaches	Not specified in excerpt	Limited to short-term horizon forecasting
J. K. Mutinda, et al. [44]	VMD-ARIMA-GRU (decomposition method)	Temperature series prediction	Better results compared to individual models	Time-consuming preprocessing	Complex preprocessing makes implementation difficult
G. Camps-Valls, et al. [45]	Deep learning technologies	Extreme climate phenomena	Training datasets lack sufficient occurrences of rare events	Not specified in excerpt	Insufficient data for extreme events
M. Bonavita [46]	Machine learning weather forecasting	Not specified	Inadequate performance during rapid temperature changes and extreme weather	Not specified in excerpt	Difficulty capturing complex non-linear relationships
R. Yang, et al. [50]	Review of machine learning techniques	Weather/climate prediction	Interpretability poses a major challenge	Not specified in excerpt	"Black box" nature restricts practical application

7. Conclusion

The research project examines deep learning predictive models through conceptual and hardware-focused advancements, which optimize temperature predictions for Iraqi meteorological zones in Dohuk, Erbil, and Mosul. The research employs three deep learning architectures, including Long Short-Term Memory (LSTM), Gated Recurrent Unit (GRU), and Artificial Neural Network (ANN), to demonstrate the outstanding abilities of LSTMs in detecting complex temporal relationships and long-term sequences, which occur naturally in climatic time series data. The LSTM models were found to achieve the highest level of RMSE, MAE, and R2 among all other models, as well as the highest level of accuracy and the lowest level of error in Dohuk, Erbil, and Mosul. The forecasting capability of LSTM models combines short-term reaction flexibility with long-term seasonal variability handling ability because of their memory-based architectural features. The GRU model was a computationally effective forecast solution, which supplied dependable predictions when one operates in hardware-restricted environments. ANN models showed poor

suitability for meteorologic forecasting because their basic feedforward design lacks the capability to track vital sequential order patterns needed for accurate predictions. These models enable practical deployment, which benefits decision-making processes based on temperature predictions throughout agriculture as well as energy management and public health and infrastructure planning sectors. The results demonstrate to stakeholders how they can establish a flexible forecasting system that works best for areas with limited resources through analyzing the model sophistication versus prediction precision and system performance. The research contributes to academia by studying deep learning applications in climate modeling for arid and semi-arid Middle Eastern areas, which have received limited scholarly attention. The research presented strong outcomes while acknowledging four main limitations involving dataset geographic restrictions to three cities and decreased model accuracy during major weather events, as well as recurrent network interpretability issues and high computational needs to train LSTM models. The study proposed several steps for future work to address current limitations and enhance model adaptability.

To achieve the best results, future researchers should combine LSTM and GRU models into hybrid approaches for higher accuracy and efficiency while using ensemble methods for improved reliability and adding environmental indicators like greenhouse gas measurements, solar radiation, and human actions to enhance contextual understanding of the predictions. Climate adaptation tools will transform into efficient mechanisms by deploying precise models that national meteorological agencies' risk assessment systems and agricultural planning platforms can use for practical implementation. Validated versions of these applications will enable district administrators to make better decisions while promoting sustainability across both Iraq and other climate-risk regions.

Acknowledgements

I extend my sincere thanks and deep gratitude to the General Authority for Meteorology and Seismic Monitoring in Baghdad for providing me with the daily observed climate data that was used to complete this research.

References

[1] J. P. Evans, “21st century climate change in the Middle East,” Clim Change, vol. 92, no. 3–4, pp. 417–432, Feb. 2009, doi: 10.1007/s10584-008-9438-5.

[2] W. H. Hassan, B. K. Nile, and B. A. Al-Masody, “Climate change effect on storm drainage networks by storm water management model,” Environmental Engineering Research, vol. 22, no. 4, pp. 393–400, Jun. 2017, doi: 10.4491/eer.2017.036.

[3] H. Chen, J. Guo, Z. Zhang, and C.-Y. Xu, “Prediction of temperature and precipitation in Sudan and South Sudan by using LARS-WG in future,” Theor Appl Climatol, vol. 113, no. 3–4, pp. 363–375, Aug. 2013, doi: 10.1007/s00704-012-0793-9.

[4] R.K. Pachauri and L.A. Meyer, “Climate Change 2014: Synthesis Report. Contribution of Working Groups I, II and III to the Fifth Assessment Report of the Intergovernmental Panel on Climate Change,” Geneva, Switzerland, 2014.

[5] M. H. Mohammed, H. M. Zwain, and W. H. Hassan, “Modeling the impacts of climate change and flooding on sanitary sewage system using SWMM simulation: A case study,” Results in Engineering, vol. 12, p. 100307, Dec. 2021, doi: 10.1016/j.rineng.2021.100307.

[6] R. J. Norby and Y. Luo, “Evaluating ecosystem responses to rising atmospheric CO 2 and global warming in a multi-factor world,” New Phytologist, vol. 162, no. 2, pp. 281–293, May 2004, doi: 10.1111/j.1469-8137.2004.01047.x.

[7] A. Al-Saegh, “Identifying a Suitable Signal Processing Technique for MI EEG Data,” Tikrit Journal of Engineering Sciences, vol. 30, no. 3, pp. 140–147, Oct. 2023, doi: 10.25130/tjes.30.3.14.

[8] A. Al-Saegh, A. Daood, and M. H. Ismail, “Dual Optimization of Deep CNN for Motor Imagery EEG Tasks Classification,” Diyala Journal of Engineering Sciences, pp. 75–91, Dec. 2024, doi: 10.24237/djes.2024.17405.

[9] Kolaib, R. J., & Waleed, J. (2024). Crime Activity Detection in Surveillance Videos Based on

Developed Deep Learning Approach. Diyala Journal of Engineering Sciences, 98-114.

[10] Flayyih, H. Q., Waleed, J., & Ibrahim, A. M. (2025). Indoor Air Quality Prediction in Sick Building Using Machine and Deep Learning: Comparative Analysis. Diyala Journal of Engineering Sciences, 203-218.

[11] K. A. Mohsen, B. K. Nile, and W. H. Hassan, "Experimental work on improving the efficiency of storm networks using a new galley design filter bucket.," IOP Conf Ser Mater Sci Eng, vol. 671, no. 1, p. 012094, Jan. 2020, doi: 10.1088/1757-899X/671/1/012094.

[12] W. H. Hassan, B. K. Nile, K. Mahdi, J. Wesseling, and C. Ritsema, "A Feasibility Assessment of Potential Artificial Recharge for Increasing Agricultural Areas in the Kerbala Desert in Iraq Using Numerical Groundwater Modeling," Water (Basel), vol. 13, no. 22, p. 3167, Nov. 2021, doi: 10.3390/w13223167.

[13] Th. O. Han, W. Z. Win and C. Th. K. Cho, "Assessment of Future Climate Change Projections Using Multiple Global Climate Models," Civil Engineering Journal, Vol. 5, No. 10, pp. 2152-2166, Oct. 2019. http://dx.doi.org/10.28991/cej-2019-03091401

[14] J. M. Eden and M. Widmann, "Downscaling of GCM-Simulated Precipitation Using Model Output Statistics," J Clim, vol. 27, no. 1, pp. 312–324, Jan. 2014, doi: 10.1175/JCLI-D-13-00063.1.

[15] E. Vanuytrecht, D. Raes, P. Willems, and M. A. Semenov, "Comparing climate change impacts on cereals based on CMIP3 and EU-ENSEMBLES climate scenarios," Agric For Meteorol, vol. 195–196, pp. 12–23, Sep. 2014, doi: 10.1016/j.agrformet.2014.04.017.

[16] W. Hassan, "Climate change projections of maximum temperatures for southwest Iraq using statistical downscaling," Clim Res, vol. 83, pp. 187–200, May 2021, doi: 10.3354/cr01647.

[17] R. L. Wilby et al., "A review of climate risk information for adaptation and development planning," International Journal of Climatology, vol. 29, no. 9, pp. 1193–1215, Jul. 2009, doi: 10.1002/joc.1839.

[18] W. H. Hassan and R. M. Khalaf, "Optimum Groundwater use Management Models by Genetic Algorithms in Karbala Desert, Iraq," IOP Conf Ser Mater Sci Eng, vol. 928, no. 2, p. 022141, Nov. 2020, doi: 10.1088/1757-899X/928/2/022141.

[19] M. N. :Khaliq, "An inventory of methods for estimating climate change-informed design water levels for floodplain mapping," 2019.

[20] M. H. Mohammed, H. M. Zwain, and W. H. Hassan, "Modeling the quality of sewage during the leaking of stormwater surface runoff to the sanitary sewer system using SWMM: a case study," Journal of Water Supply: Research and Technology-Aqua, vol. 71, no. 1, pp. 86–99, Jan. 2022, doi: 10.2166/aqua.2021.227.

[21] H. K. Jalal and W. H. Hassan, "Three-dimensional numerical simulation of local scour around circular bridge pier using Flow-3D software," IOP Conf Ser Mater Sci Eng, vol. 745, p. 012150, Mar. 2020, doi: 10.1088/1757-899X/745/1/012150.

[22] Z. Xu, Y. Han, and Z. Yang, "Dynamical downscaling of regional climate: A review of methods and limitations," Sci China Earth Sci, vol. 62, no. 2, pp. 365–375, Feb. 2019, doi: 10.1007/s11430-018-9261-5.

[23] H.-I. Eum, A. Gupta, and Y. Dibike, "Effects of univariate and multivariate statistical downscaling methods on climatic and hydrologic indicators for Alberta, Canada," J Hydrol (Amst), vol. 588, p. 125065, Sep. 2020, doi: 10.1016/j.jhydrol.2020.125065.

[24] C.-Y. Lee, S. J. Camargo, A. H. Sobel, and M. K. Tippett, "Statistical–Dynamical Downscaling Projections of Tropical Cyclone Activity in a Warming Climate: Two Diverging Genesis Scenarios," J Clim, vol. 33, no. 11, pp. 4815–4834, Jun. 2020, doi: 10.1175/JCLI-D-19-0452.1.

[25] W. H. Hassan, Z. H. Attea, and S. S. Mohammed, "Optimum layout design of sewer networks by hybrid genetic algorithm," Journal of Applied Water Engineering and Research, vol. 8, no. 2, pp. 108–124, Apr. 2020, doi: 10.1080/23249676.2020.1761897.

[26] S. A. Adachi and H. Tomita, "Methodology of the Constraint Condition in Dynamical Downscaling for Regional Climate Evaluation: A Review," Journal of Geophysical Research: Atmospheres, vol. 125, no. 11, Jun. 2020, doi: 10.1029/2019JD032166.

[27] W. H. Hassan et al., "Effect of Artificial (Pond) Recharge on the Salinity and Groundwater Level in Al-Dibdibba Aquifer in Iraq Using Treated Wastewater," Water (Basel), vol. 15, no. 4, p. 695, Feb. 2023, doi: 10.3390/w15040695.

[28] A. M. Rasheed, "Adaptation of Water Sensitive Urban Design to Climate Change," Queensland University of Technology, 2018. doi: 10.5204/thesis.eprints.122960.

[29] W. H. Hassan, H. H. Hussein, M. H. Alshammari, H. K. Jalal, and S. E. Rasheed, "Evaluation of gene expression programming and artificial neural networks in PyTorch for the prediction of local scour depth around a bridge pier," Results in

Engineering, vol. 13, p. 100353, Mar. 2022, doi: 10.1016/j.rineng.2022.100353.

[30] M. Z. Hashmi, A. Y. Shamseldin, and B. W. Melville, "Comparison of SDSM and LARS-WG for simulation and downscaling of extreme precipitation events in a watershed," Stochastic Environmental Research and Risk Assessment, vol. 25, no. 4, pp. 475–484, May 2011, doi: 10.1007/s00477-010-0416-x.

[31] M. A. Semenov and E. M. Barrow, "LARS-WG A Stochastic Weather Generator for Use in Climate Impact Studies," 2002.

[32] R. L. Wilby and C. W. Dawson, "Using SDSM Version 3.1-A decision support tool for the assessment of regional climate change impacts User Manual Sponsors of SDSM A Consortium for the Application of Climate Impact Assessments (ACACIA) Canadian Climate Impacts Scenarios (CCIS) Project Environment Agency of England and Wales," 2004.

[33] S. L. Zubaidi, P. Kot, K. Hashim, R. Alkhaddar, M. Abdellatif, and Y. R. Muhsin, "Using LARS –WG model for prediction of temperature in Columbia City, USA," IOP Conf Ser Mater Sci Eng, vol. 584, no. 1, p. 012026, Aug. 2019, doi: 10.1088/1757-899X/584/1/012026.

[34] M. Costa-Cabral et al., "Climate variability and change in mountain environments: some implications for water resources and water quality in the Sierra Nevada (USA)," Clim Change, vol. 116, no. 1, pp. 1–14, Jan. 2013, doi: 10.1007/s10584-012-0630-2.

[35] H. Birara, R. P. Pandey, and S. K. Mishra, "Projections of future rainfall and temperature using statistical downscaling techniques in Tana Basin, Ethiopia," Sustain Water Resour Manag, vol. 6, no. 5, p. 77, Oct. 2020, doi: 10.1007/s40899-020-00436-1.

[36] I. Hassan, R. M. Kalin, C. J. White, and J. A. Aladejana, "Selection of CMIP5 GCM Ensemble for the Projection of Spatio-Temporal Changes in Precipitation and Temperature over the Niger Delta, Nigeria," Water (Basel), vol. 12, no. 2, p. 385, Feb. 2020, doi: 10.3390/w12020385.

[37] C. B. Chisanga, E. Phiri, and V. R. N. Chinene, "Reliability of Rain-Fed Maize Yield Simulation Using LARS-WG Derived CMIP5 Climate Data at Mount Makulu, Zambia," Journal of Agricultural Science, vol. 12, no. 11, p. 275, Oct. 2020, doi: 10.5539/jas.v12n11p275.

[38] W. T. Hailesilassie, N. K. Goel, T. Ayenew, and S. Tekleab, "Future precipitation changes in the Central Ethiopian Main Rift under CMIP5 GCMs," Journal of Water and Climate Change, vol. 13, no. 4, pp. 1830–1841, Apr. 2022, doi: 10.2166/wcc.2022.440.

[39] N. Saddique, C. Bernhofer, R. Kronenberg, and M. Usman, "Downscaling of CMIP5 Models Output by Using Statistical Models in a Data Scarce Mountain Environment (Mangla Dam Watershed), Northern Pakistan," Asia Pac J Atmos Sci, vol. 55, no. 4, pp. 719–735, Nov. 2019, doi: 10.1007/s13143-019-00111-2.

[40] S. Punyawansiri and B. Kwanyuen, "Forecasting the Future Temperature Using a Downscaling Method by LARS-WG Stochastic Weather Generator at the Local Site of Phitsanulok Province, Thailand," Atmospheric and Climate Sciences, vol. 10, no. 04, pp. 538–552, 2020, doi: 10.4236/acs.2020.104028.

[41] H. Algretawee, R. J. M. Al-Saadi, M. F. Al Juboury, W. H. Hasan, B. K. Nile, and M. A. Kadhim, "Determination of Difference Amount in Reference Evapotranspiration between Urban and Suburban Quarters in Karbala City," Journal of Ecological Engineering, vol. 23, no. 7, pp. 180–191, Jul. 2022, doi: 10.12911/22998993/149720.

[42] X. Fan, L. Jiang, and J. Gou, "Statistical downscaling and projection of future temperatures across the Loess Plateau, China," Weather Clim Extrem, vol. 32, p. 100328, Jun. 2021, doi: 10.1016/j.wace.2021.100328.

[43] S. Doulabian, S. Golian, A. S. Toosi, and C. Murphy, "Evaluating the effects of climate change on precipitation and temperature for Iran using RCP scenarios," Journal of Water and Climate Change, vol. 12, no. 1, pp. 166–184, Feb. 2021, doi: 10.2166/wcc.2020.114.

[44] Z. Karevan and J. A. K. Suykens, "Transductive LSTM for time-series prediction: An application to weather forecasting," Neural Networks, vol. 125, pp. 1–9, May 2020, doi: 10.1016/j.neunet.2019.12.030.

[45] Q. Guo, Z. He, Z. Wang, S. Qiao, J. Zhu, and J. Chen, "A Performance Comparison Study on Climate Prediction in Weifang City Using Different Deep Learning Models," Water (Basel), vol. 16, no. 19, p. 2870, Oct. 2024, doi: 10.3390/w16192870.

[46] J. K. Mutinda, A. K. Langat, and S. M. Mwalili, "Forecasting Temperature Time Series Data Using Combined Statistical and Deep Learning Methods: A Case Study of Nairobi County Daily Temperature," Int J Math Math Sci, vol. 2025, no. 1, Jan. 2025, doi: 10.1155/ijmm/4795841.

[47] G. Camps-Valls et al., "Artificial intelligence for modeling and understanding extreme weather and climate events," Nat Commun, vol. 16, no. 1, p. 1919, Feb. 2025, doi: 10.1038/s41467-025-56573-8.

[48] M. Bonavita, "On Some Limitations of Current Machine Learning Weather Prediction Models," Geophys Res Lett, vol. 51, no. 12, Jun. 2024, doi: 10.1029/2023GL107377.

[49] A. E. Abdelkareem, "Performance Analysis of Deep Learning based Signal Constellation Identification Algorithms for Underwater Acoustic Communications," Diyala Journal of Engineering Sciences, pp. 1–14, Sep. 2024, doi: 10.24237/djes.2024.17301.

[50] R. Yang et al., "Interpretable machine learning for weather and climate prediction: A review," Atmos Environ, vol. 338, p. 120797, Dec. 2024, doi: 10.1016/j.atmosenv.2024.120797.